

## Excitation of $^9F$ Levels of Gadolinium Atom Belonging to $4f^75d6s6p$ Configuration

Yuriy M. Smirnov

National Research University, Moscow Power Engineering Institute,

14 Krasnokazarmennaya str., Moscow, 111250, Russia

SmirnovYM@mpei.ru

### Abstract

The excitation of  $^9F$  levels of gadolinium atoms related to the  $4f^75d6s6p$  configuration was examined by the method of extended crossing beams with the registration of the excited atom radiation. 68 excitation cross sections were measured at the incident electron energy of 30 eV. Optical excitation functions (OEF) in the electron energy range 0-200 eV were recorded for transitions from 13 levels. The direct excitation channel as well as the OEF features are discussed. A comparison with the results of an earlier experiment is given.

**Keywords:** Excitation Cross-Section, Optical Excitation Function, Gadolinium Atom, Energy Level, Spectral Line, Nonet Levels

### 1. INTRODUCTION

Gadolinium was discovered in 1880 by the Swiss scientist J. S. G. de Marignac; like almost all rare earth elements, gadolinium did not find any practical applications for several decades. However, in the first half of the twentieth century, researchers have discovered some unique gadolinium properties.

First, gadolinium has the largest thermal neutron capture cross-section among all elements, which is a prerequisite for its use in nuclear power. Secondly, gadolinium is a ferromagnetic, and even stronger than nickel and cobalt. Unfortunately, gadolinium is ferromagnetic at  $T \leq 290$  K (17° C), while nickel retains ferromagnetic properties up to  $T = 631$  K, and cobalt and iron up to  $T \approx 1000$  K. Magnetic properties of some gadolinium compounds are also unusual. In addition, at low temperatures, gadolinium alloy with cerium and ruthenium becomes superconducting and however retains weak ferromagnetism. Third, gadolinium is characterized by good compatibility with the components of ferrous metals, as well as with titanium. Gadolinium is used to improve the properties of titanium (if necessary). Fourth, some gadolinium-based materials are of great interest for optoelectronics.

It should also be noted the importance of information on the spectra and atomic characteristics of gadolinium atom and ions (GdI, GdII, GdIII) in solving a number of problems of astrophysics. In particular, the study of roAp stars found that the content of gadolinium in their atmospheres exceeds the content of gadolinium in the sun's atmosphere by two orders of magnitude (in stars HD 122970, 10 Aql [1]; HD 24712 [2]) and even by three orders of magnitude (in star HD 101065 [2]). In all these cases, the content of gadolinium is determined by the GdII spectrum. "Furthermore, we corroborate the characteristics of roAp stars that second ions of REE are overabundant by a factor of up to 100 (!) compared to values derived from singly ionized species" [1]. At solving problems related to the determination of atmospheric characteristics of roAp stars, mathematical modeling was widely used, which requires reliable and complete information about the spectra and atomic constants of atoms and ions. "The next step in modeling the photosphere of HD 101065 must once more be to extend the basis for realistic opacity calculations. Suitable data for the second ionization stage of REEs are still scarce and data on neutral atoms and first ions of the REEs are still fairly incomplete" [2].

The atomic constants characterizing inelastic collisions of electrons with atoms (excitation cross-sections) are studied much less than the radiation characteristics (transition probabilities, oscillator forces). In particular, the excitation cross-sections of gadolinium atom by electron impact were initially investigated only in [3]. At the

same time, the author of the work [3] points out: "The study of excitation of gadolinium atoms in the free state by electron impact is associated with overcoming *huge experimental difficulties*" (emphasis is mine). In a later work [4] the excitation of the GdI undecuplet levels belonging to  $4f^7 5d^2 6p$  configuration was studied, and then in [5] the excitation cross sections for the GdI quintet and septet levels belonging to  $4f^8 5d 6s$  configuration was determined.

In this paper, the excitation of spontaneous transitions of the gadolinium atom from the upper  $^9F$  levels related to the  $4f^7 5d 6s 6p$  configuration is studied in detail. The method of extended crossing beams is used. Earlier, when discussing the technique and methodology of the experiment (for example, [6, 7]), it was noted that this method has practically no restrictions in the area of examined objects at the study of electron-atomic collisions.

## 2. MAIN EXPERIMENTAL CONDITIONS

Since the technique and methods of experiments with extended crossing beams have been discussed in detail in recent papers [6, 7], the repetition of these discussions in this paper is unnecessary. It is sufficiently to specify only the basic conditions for experiments with gadolinium.

Gadolinium of 99.93% purity (the main impurities of terbium and yttrium with a content of 0.01%) was heated by an electron ray of the melting electron gun to a temperature  $T = 1860$  K, exceeding its melting temperature by  $\Delta T = 260$  K. Due to this, the molten zone was wide enough and had a stable surface throughout the experiment. At the above-mentioned temperature (in the main part of the experiment), the atom concentration in the intersection zone of the atomic and electron beams was  $n = 1.2 \times 10^{10} \text{ cm}^{-3}$ . Since the most intense of the studied transitions ended on the levels of the main term  $4f^7 5d 6s^2 \ ^9D^\circ$ , the concentration of atoms was reduced to  $\sim 10^9 \text{ cm}^{-3}$  to minimize reabsorption.

Although the ground term  $4f^7 ({}^8S^\circ) 5d 6s^2 \ ^9D^\circ$  of the gadolinium atom is nonet, it contains not nine, but only five levels, since it is a  $D$  term. The  $J$  splitting of the ground term is relatively small; in addition, ground term of GdI has a direct order of levels, it means, that the highest level has the greatest value  $J = 6$ . The estimation of the level population of the ground term at the above-mentioned evaporation temperature gives the following values (in % of the total atom number in the beam; in brackets is given the level energy in  $\text{cm}^{-1}$ ):  $J = 2$  (0) – 19.4; 3 (215) – 23.1; 4 (532) – 23.1; 5 (999) – 19.7; 6 (1719) – 13.2. Thus, the presence of a direct order of levels leads to a significant equalization of the ground term level populations. The closest to the ground term is the odd undecuplet term  $4f^7 ({}^8S^\circ) 5d^2 ({}^3F) ({}^{10}F^\circ) 6s \ ^{11}F^\circ$  ( $E = 6478\text{--}8498 \text{ cm}^{-1}$ ), the total population of which is about 1%; it overlaps with the levels of the septet term  $4f^7 ({}^8S^\circ) 5d 6s^2 \ ^7D^\circ$  ( $E = 6976\text{--}7653 \text{ cm}^{-1}$ ), having a total population of only 0.5%. Thus, the excitation of the upper  $^9F$  levels, studied in the present work, comes from the five initial levels of the ground term, the population of which have a little difference. This fact should be taken into account when comparing the experimental values of the cross-sections with the theoretical ones (in the case of appearance the latter). Previously, such accounting for a number of other metal atoms was performed in the theoretical works of R. K. Peterkop (for example, [8]).

The current density of the electron beam in the entire operating range of electron energies  $E = 0\text{--}200$  eV did not exceed  $1.0 \text{ mA/cm}^2$ . The spectral resolution of the installation was about 0.1 nm in the wavelength range  $\lambda = 190\text{--}630$  nm and about 0.2 nm at  $\lambda > 600$  nm (in the main operating mode). If necessary, some parts of the spectrum were recorded with a resolution of up to 0.05 nm. The measurement error of the cross-section relative values was 3-8% depending on the intensity of the line and its location in the spectrum. The absolute values of the cross-sections are determined with an error of 20-25%.

## 3. RESULTS AND DISCUSSION

The optical emission spectrum resulting from collisions of monoenergetic electrons ( $E = 30$  eV) with gadolinium atoms is registered in the wavelength range  $\lambda = 190\text{--}853$  nm. However, the GdI spectrum is present only on part with  $\lambda = 300\text{--}853$  nm, whereas all the lines at the shorter wavelengths is related to the spectrum of GdII. For

sufficiently intense GdI lines, the dependence of the cross sections on the energy of the incident electrons (optical excitation functions, OEFs) in the electron energy range  $E = 0\text{--}200$  eV was recorded.

The results obtained with the addition of the necessary background information about the wavelengths and transition parameters are presented in the table 1. Here are the wavelengths  $\lambda$ , transitions, the values of the internal quantum number for the lower  $J_{\text{low}}$  and upper  $J_{\text{up}}$  levels, the energy of the lower  $E_{\text{low}}$  and upper  $E_{\text{up}}$  levels, the excitation cross-sections at the electron energy of 30 eV  $Q_{30}$ , the values of the cross sections in the OEF maximum  $Q_{\text{max}}$ , the position of the maximum  $E(Q_{\text{max}})$ . The OEF column shows the OEF numbers according to the curve numbering in figure 1. The format of figure 1 usual for representation of atomic OEFs: the scale on the abscissa axis is logarithmic, on the ordinate axis is linear with an individual level of zero reference for each curve. All curves are normalized to one at the maximum and arranged in such a way as to avoid their intersection or contact.

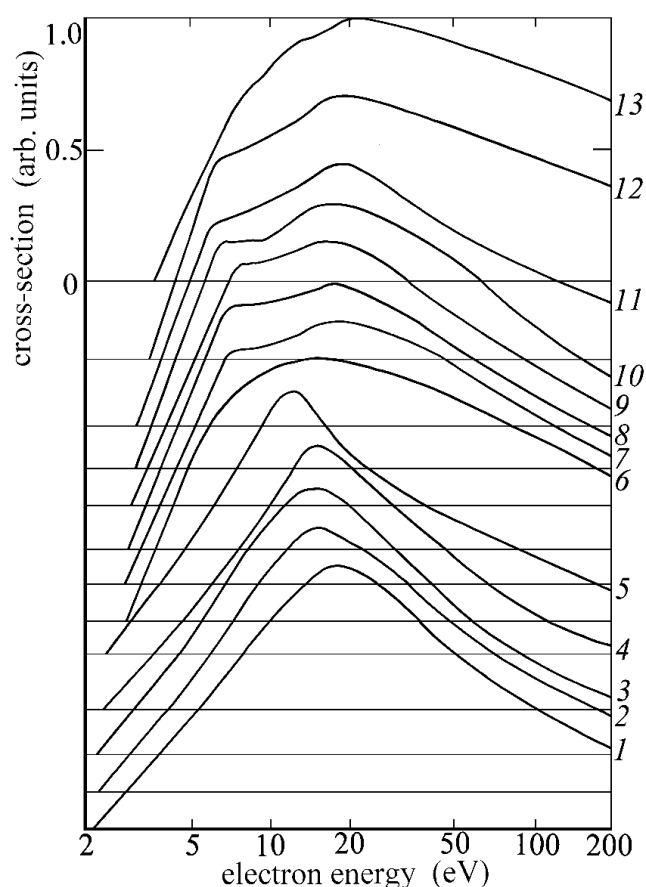


**Figure 1.** Optical excitation functions of gadolinium atom.

Reference data on the characteristics of the GdI energy levels are mainly taken from [9], taking into account the results of [10, 11], in which the isotope shift for several tens of GdI lines is studied and on the basis of these data the configuration for a number of even levels is determined. The last two papers have been published relatively recently, but they have not brought complete clarity to the configuration definition for  ${}^9F$  levels. In work [9], two groups of lines are given for which only the term  ${}^9F$  is specified, and the configuration is unknown. Although they are given as nonet terms, both groups contain only seven levels because they are  $F$  terms. The first group is located in the energy range  $E = 26145\text{--}27336$   $\text{cm}^{-1}$ , and the second in the range  $E = 28504\text{--}29717$   $\text{cm}^{-1}$ . In work [11] for three levels from the first group the  $4f^85d6s$  configuration is offered (for other four levels the configuration is not defined), and for all seven levels of the second group –  $4f^75d6s6p$ , which is a subject of

consideration in the present work. Five levels from the second group are present in table 1 in the present paper. The configurations given in the table 1 according to [9], indicate the states in which the subshells are found, whereas for the levels from [10, 11] the configuration is given as  $4f^7 5d 6s 6p$ , since a detailed theoretical analysis of the subshell states was not carried out in [10, 11]. At the same time, there is no doubt that the subshell  $4f^7$  is in the state ( $^8S^\circ$ ).

It should be noted that for levels  $4f^7(^8S^\circ)5d(^9D^\circ)6s6p(^3P^\circ) ^9F$  mixing of configurations is relatively small (only for one level the content of the main component is less than 50%), while the levels  $4f^7(^8S^\circ)5d(^9D^\circ)6s6p(^1P^\circ) ^9F$  are characterized by a very strong mixing: for levels with  $J = 2-6$  the content of the main component is within 20–25%, while the first impurity component relates to the configuration  $4f^7(^8S^\circ)5d(^3F) (^{10}F^\circ)6p$  and has a content in the range of 17–25% (terms  $^9F$  and  $^{11}G$ ). Thus, for levels  $4f^7(^8S^\circ)5d(^9D^\circ)6s6p(^1P^\circ) ^9F$ , the unambiguous indication of the configuration is largely conditional. When considering the OEFs depicted in figure 1, attention is drawn to the fact that OEFs are divided in form into two groups: OEFs №1–5 and 6–13. This separation is consistent with the assignment of upper levels to subconfigurations  $4f^7(^8S^\circ)5d(^9D^\circ)6s6p(^3P^\circ)$  and  $4f^7(^8S^\circ)5d(^9D^\circ)6s6p(^1P^\circ)$ , respectively.

In four cases, there is a blending; blends are highlighted in the table 1 by horizontal lines. Summary cross-sections  $Q_{30}$  were measured for blends, because the spectral resolution of our installation is not enough for hardware separation of closely spaced lines. However, the excitation cross sections of the blend components can be determined by calculation, if we use branching factors based on the results of [12], devoted to the measurement of transition probabilities in the GdI spectrum. The results obtained by this procedure are noted in the table 1 by asterisks.

**Table 1.** Excitation cross-sections of gadolinium atom

$\lambda$ (nm)	Transition	$J_{low}$ $-J_{up}$	$E_{low}$ ( $cm^{-1}$ )	$E_{up}$ ( $cm^{-1}$ )	$Q_{30}$ ( $10^{-18}$ $cm^2$ )	$Q_{max}$ ( $10^{-18}$ $cm^2$ )	$E(Q_{max})$ (eV)	OEF
(338.197 338.223)	$4f^7 5d 6s^2 ^9D^\circ - ?$ $(4f^7 5d 6s^2 ^9D^\circ - 4f^7 5d 6s 6p ^9F)$	6–5 2–1	1719 0	31279 29557)	0.75	-	-	-
339.722 339.733	$4f^7 5d 6s^2 ^9D^\circ - 4f^7 5d^2 6p ^{11}D$ $4f^7 5d 6s^2 ^9D^\circ - 4f^7 5d 6s 6p ^9F$	6–7 2–3	1719 0	31146 29426	0.55* 1.37*	-	-	-
342.235	$4f^7 5d 6s^2 ^9D^\circ - 4f^7 5d 6s 6p ^9F$	3–3	215	29426	1.03	-	-	-
349.710	$4f^7 5d 6s^2 ^9D^\circ - 4f^7 5d 6s 6p ^9F$	4–5	532	29119	1.04	1.08	22	13
349.816	$4f^7 5d 6s^2 ^9D^\circ - 4f^7 5d 6s 6p ^9F$	3–4	215	28793	1.08	-	-	-
353.751	$4f^7 5d 6s^2 ^9D^\circ - 4f^7 5d 6s 6p ^9F$	4–4	532	28793	1.51	-	-	-
359.684	$4f^7 5d 6s^2 ^9D^\circ - 4f^7 5d 6s 6p ^9F$	5–4	999	28793	2.25	-	-	-
364.848	$4f^7 5d 6s^2 ^9D^\circ - 4f^7 5d 6s 6p ^9F$	6–5	1719	29119	3.06	3.16	22	13
373.232	$4f^7 5d 6s^2 ^9D^\circ - 4f^7 5d 6s 6p ^9F$	6–7	1719	28504	3.45	3.61	19	12
422.585	$4f^7 5d 6s^2 ^9D^\circ - 4f^7 5d(^9D^\circ)6s6p(^1P^\circ) ^9F$	6–7	1719	25376	91.4	102.	19	11
426.012	$4f^7 5d 6s^2 ^9D^\circ - 4f^7 5d(^9D^\circ)6s6p(^1P^\circ) ^9F$	4–5	532	23999	26.6	30.2	16	9

426.659	$4f^7 5d 6s^2 {}^9D^\circ - 4f^7 5d ({}^9D^\circ) 6s 6p ({}^1P^\circ) {}^9F$	5-6	999	24430	13.1*	14.2	16	10
426.701	$4f^7 5d 6s^2 {}^9D^\circ - 4f^7 5d ({}^9D^\circ) 6s 6p ({}^1P^\circ) {}^9F$	3-4	215	23644	15.4*	16.9	17	8
427.417	$4f^7 5d 6s^2 {}^9D^\circ - 4f^7 5d ({}^9D^\circ) 6s 6p ({}^1P^\circ) {}^9F$	2-3	0	23389	12.1	12.9	19	7
430.634	$4f^7 5d 6s^2 {}^9D^\circ - 4f^7 5d ({}^9D^\circ) 6s 6p ({}^1P^\circ) {}^9F$	2-2	0	23215	46.0	49.0	15	6
431.384	$4f^7 5d 6s^2 {}^9D^\circ - 4f^7 5d ({}^9D^\circ) 6s 6p ({}^1P^\circ) {}^9F$	3-3	215	23389	78.8	83.8	19	7
432.569	$4f^7 5d 6s^2 {}^9D^\circ - 4f^7 5d ({}^9D^\circ) 6s 6p ({}^1P^\circ) {}^9F$	4-4	532	23644	90.0	98.6	17	8
433.749	$4f^7 5d^2 6s {}^{11}F^\circ - 4f^7 5d 6s 6p {}^9F$	2-3	6378	29426	4.45	-	-	-
434.645	$4f^7 5d 6s^2 {}^9D^\circ - 4f^7 5d ({}^9D^\circ) 6s 6p ({}^1P^\circ) {}^9F$	5-5	999	23999	134.*	152.	16	9
434.662	$4f^7 5d 6s^2 {}^9D^\circ - 4f^7 5d ({}^9D^\circ) 6s 6p ({}^1P^\circ) {}^9F$	3-2	215	23215	52.2*	55.6	15	6
437.015	$4f^7 5d^2 6s {}^{11}F^\circ - 4f^7 5d 6s 6p {}^9F$	3-3	6550	29426	2.68	-	-	-
437.384	$4f^7 5d 6s^2 {}^9D^\circ - 4f^7 5d ({}^9D^\circ) 6s 6p ({}^1P^\circ) {}^9F$	4-3	532	23389	48.5	51.6	19	7
440.185	$4f^7 5d 6s^2 {}^9D^\circ - 4f^7 5d ({}^9D^\circ) 6s 6p ({}^1P^\circ) {}^9F$	6-6	1719	24430	42.5	46.2	16	10
441.474	$4f^7 5d 6s^2 {}^9D^\circ - 4f^7 5d ({}^9D^\circ) 6s 6p ({}^1P^\circ) {}^9F$	5-4	999	23644	32.8	36.0	17	8
441.567	$4f^7 5d^2 6s {}^{11}F^\circ - 4f^7 5d 6s 6p {}^9F$	4-3	6786	29426	1.01	-	-	-
448.690	$4f^7 5d 6s^2 {}^9D^\circ - 4f^7 5d ({}^9D^\circ) 6s 6p ({}^1P^\circ) {}^9F$	6-5	1719	23999	19.6	22.2	16	9
450.496	$4f^7 5d 6s^2 {}^7D^\circ - 4f^7 5d 6s 6p {}^9F$	4-3	7234	29426	1.47	-	-	-
454.423	$4f^7 5d 6s^2 {}^7D^\circ - 4f^7 5d 6s 6p {}^9F$	3-3	7426	29426	2.55	-	-	-
457.245	$4f^7 5d 6s^2 {}^7D^\circ - 4f^7 5d 6s 6p {}^9F$	2-3	7562	29426	0.95	-	-	-
458.233	$4f^7 5d 6s^2 {}^7D^\circ - 4f^7 5d 6s 6p {}^9F$	5-4	6976	28793	1.51	-	-	-
486.313	$4f^7 5d^2 6s {}^{11}F^\circ - 4f^7 5d 6s 6p {}^9F$	7-7	7947	28504	0.41	0.43	19	12
524.333	$4f^7 5d^2 6s {}^9F^\circ - 4f^7 5d 6s 6p {}^9F$	2-3	10359	29426	0.58	-	-	-
534.181	$4f^7 5d 6s^2 {}^9D^\circ - 4f^7 5d ({}^9D^\circ) 6s 6p ({}^3P^\circ) {}^9F$	6-7	1719	20434	2.93	4.65	12	5
548.200	$4f^7 5d^2 6s {}^9F^\circ - 4f^7 5d 6s 6p {}^9F$	4-5	10883	29119	0.61	0.63	22	13
558.196	$4f^7 5d^2 6s {}^9F^\circ - 4f^7 5d 6s 6p {}^9F$	4-4	10883	28793	0.53	-	-	-
558.630	$4f^7 5d^2 6s {}^{11}F^\circ - 4f^7 5d ({}^9D^\circ) 6s 6p ({}^1P^\circ) {}^9F$	6-7	7480	25376	0.94	1.05	19	11
562.955	$4f^7 5d 6s^2 {}^9D^\circ - 4f^7 5d ({}^9D^\circ) 6s 6p ({}^3P^\circ) {}^9F$	3-4	215	17973	7.50	9.75	15	4
567.453	$4f^7 5d 6s^2 {}^9D^\circ - 4f^7 5d ({}^9D^\circ) 6s 6p ({}^3P^\circ) {}^9F$	2-3	0	17617	0.23	0.31	15	3
570.942	$4f^7 5d 6s^2 {}^9D^\circ - 4f^7 5d ({}^9D^\circ) 6s 6p ({}^3P^\circ) {}^9F$	5-5	999	18509	4.47	-	-	-

573.216	$4f^7 5d 6s^2 {}^9D^\circ - 4f^7 5d ({}^9D^\circ) 6s 6p ({}^3P^\circ) {}^9F$	4-4	532	17973	2.74	3.56	15	4
573.597	$4f^7 5d^2 6s {}^{11}F^\circ - 4f^7 5d ({}^9D^\circ) 6s 6p ({}^1P^\circ) {}^9F$	7-7	7947	25376	1.43	1.59	19	11
574.466	$4f^7 5d 6s^2 {}^9D^\circ - 4f^7 5d ({}^9D^\circ) 6s 6p ({}^3P^\circ) {}^9F$	3-3	215	17617	3.86	5.12	15	3
575.188	$4f^7 5d 6s^2 {}^9D^\circ - 4f^7 5d ({}^9D^\circ) 6s 6p ({}^3P^\circ) {}^9F$	2-2	0	17380	4.92	6.00	15	2
576.974	$4f^7 5d^2 6s {}^{11}F^\circ - 4f^7 5d ({}^9D^\circ) 6s 6p ({}^1P^\circ) {}^9F$	5-6	7103	24430	0.97	1.05	16	10
578.223	$4f^7 5d^2 6s {}^9F^\circ - 4f^7 5d 6s 6p {}^9F$	6-5	11830	29119	0.18	0.18	22	13
580.292	$4f^7 5d 6s^2 {}^9D^\circ - 4f^7 5d ({}^9D^\circ) 6s 6p ({}^3P^\circ) {}^9F$	2-1	0	17227	7.64	8.79	18	1
580.771	$4f^7 5d^2 6s {}^{11}F^\circ - 4f^7 5d ({}^9D^\circ) 6s 6p ({}^1P^\circ) {}^9F$	4-5	6786	23999	2.53	2.88	16	9
582.397	$4f^7 5d 6s^2 {}^9D^\circ - 4f^7 5d ({}^9D^\circ) 6s 6p ({}^3P^\circ) {}^9F$	3-2	215	17380	4.88	5.95	15	2
(584.367	$4f^7 5d^2 6s {}^{11}P^\circ - 4f^7 5d 6s 6p {}^9F$	4-4	11685	28793)	0.32	-	-	-
584.847	$4f^7 5d^2 6s {}^{11}F^\circ - 4f^7 5d ({}^9D^\circ) 6s 6p ({}^1P^\circ) {}^9F$	3-4	6550	23644	1.96	2.15	17	8
587.670	$4f^7 5d^2 6s {}^{11}F^\circ - 4f^7 5d ({}^9D^\circ) 6s 6p ({}^1P^\circ) {}^9F$	2-3	6378	23389	1.25	1.33	19	7
589.804	$4f^7 5d^2 6s {}^{11}F^\circ - 4f^7 5d ({}^9D^\circ) 6s 6p ({}^1P^\circ) {}^9F$	6-6	7480	24430	0.82	0.90	16	10
591.677	$4f^7 5d^2 6s {}^{11}F^\circ - 4f^7 5d ({}^9D^\circ) 6s 6p ({}^1P^\circ) {}^9F$	5-5	7103	23999	2.77	3.15	16	9
593.027	$4f^7 5d^2 6s {}^{11}F^\circ - 4f^7 5d ({}^9D^\circ) 6s 6p ({}^1P^\circ) {}^9F$	4-4	6786	23644	6.35	6.98	17	8
593.681	$4f^7 5d^2 6s {}^{11}F^\circ - 4f^7 5d ({}^9D^\circ) 6s 6p ({}^1P^\circ) {}^9F$	3-3	6550	23389	7.07	7.52	19	7
593.771	$4f^7 5d^2 6s {}^{11}F^\circ - 4f^7 5d ({}^9D^\circ) 6s 6p ({}^1P^\circ) {}^9F$	2-2	6378	23215	4.13	4.40	15	6
596.315	$4f^7 5d 6s^2 {}^7D^\circ - 4f^7 5d ({}^9D^\circ) 6s 6p ({}^1P^\circ) {}^9F$	4-5	7234	23999	1.48	1.68	16	9
(597.341	$4f^7 5d^2 6s {}^{11}P^\circ - 4f^7 5d 6s 6p {}^9F$	5-4	12057	28793)	0.51	-	-	-
599.907	$4f^7 5d^2 6s {}^{11}F^\circ - 4f^7 5d ({}^9D^\circ) 6s 6p ({}^1P^\circ) {}^9F$	3-2	6550	23215	4.94	5.26	15	6
602.112	$4f^7 5d^2 6s {}^{11}F^\circ - 4f^7 5d ({}^9D^\circ) 6s 6p ({}^1P^\circ) {}^9F$	4-3	6786	23389	3.07	3.26	19	7
604.401	$4f^7 5d^2 6s {}^{11}F^\circ - 4f^7 5d ({}^9D^\circ) 6s 6p ({}^1P^\circ) {}^9F$	5-4	7103	23644	0.58	0.64	17	8
642.452	$4f^7 5d 6s^2 {}^7D^\circ - 4f^7 5d ({}^9D^\circ) 6s 6p ({}^1P^\circ) {}^9F$	1-2	7653	23215	1.23	1.31	15	6
(753.134	$4f^7 5d^2 6s {}^9P^\circ - 4f^7 5d 6s 6p {}^9F$	4-4	15519	28793)	0.57	-	-	-
762.194	$4f^7 5d^2 6s {}^9F^\circ - 4f^7 5d ({}^9D^\circ) 6s 6p ({}^1P^\circ) {}^9F$	4-5	10883	23999	3.16	3.60	16	9
765.032	$4f^7 5d^2 6s {}^9F^\circ - 4f^7 5d ({}^9D^\circ) 6s 6p ({}^1P^\circ) {}^9F$	3-4	10576	23644	2.83	3.11	17	8
767.256	$4f^7 5d^2 6s {}^9F^\circ - 4f^7 5d ({}^9D^\circ) 6s 6p ({}^1P^\circ) {}^9F$	2-3	10359	23389	2.92	3.10	19	7

769.446	$4f^7 5d^2 6s^9 F^{\circ} - 4f^7 5d(^9 D^{\circ}) 6s 6p(^1 P^{\circ})^9 F$	1-2	10222	23215	1.77	1.88	15	6
783.443	$4f^7 5d^2 6s^9 F^{\circ} - 4f^7 5d(^9 D^{\circ}) 6s 6p(^1 P^{\circ})^9 F$	4-4	10883	23644	0.58	0.64	17	8
799.560	$4f^7 5d 6s^2 ^7 D^{\circ} - 4f^7 5d(^9 D^{\circ}) 6s 6p(^3 P^{\circ})^9 F$	5-6	6976	19480	5.40	-	-	-

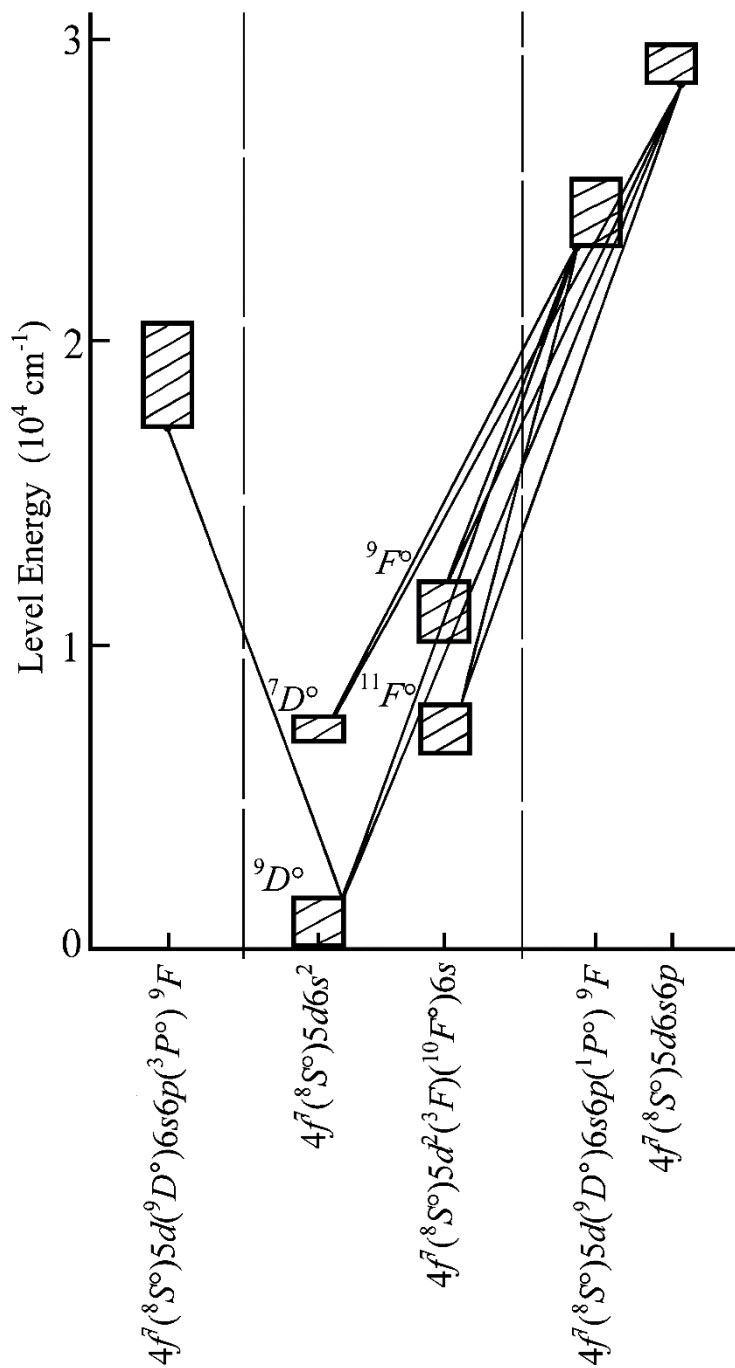


**Figure 2.** Partial state diagram of gadolinium atom.

Several lines registered on our spectrogram are absent in all spectroscopic sources available to the author. The most likely reason for this is that the most detailed gadolinium spectrum data obtained using gas-discharge radiation sources at very high spectral resolution are only partially published, as for other REEs. For these lines, within the framework of this work, a classification is undertaken using the GdI level system published in [9]. The results are presented in table 1 in parentheses in columns 1–5. As can be seen, three such transitions, located in the yellow-red part of the spectrum, occur from the upper-level  $E = 28793 \text{ cm}^{-1}$ ; for another upper level  $E = 31279 \text{ cm}^{-1}$  neither configuration nor term is known (in the second column it is marked with a question mark).

A partial diagram of the gadolinium atom states with the transitions studied is shown in figure 2. Vertical dashed lines separate states with different parity. To simplify the picture, the terms are represented by blocks without specifying splitting by  $J$ , so each combination of the two blocks corresponds to a multiplet, not an individual transition. The configuration symbols for all states, as well as the terms for the upper levels, are placed under the abscissa axis. The term symbols for the lower (odd) levels are placed on the picture field next to the corresponding blocks.

The excitation of the levels studied in this paper is due to changes affecting only the most outer electron shell of  $6s^2$ , while the more deeply located shells of  $4f^7$  and  $5d$  remain unchanged. Thus, there is a allowed one-electron transition of one of the equivalent  $6s$  electrons  $6s \rightarrow 6p$ , the transition probability of which can be quite high due to the absence of forbiddances. As seen in table 1, the excitation cross sections of transitions from  $4f^7 5d(^9D^\circ) 6s 6p(^1P^\circ)$  sub-configuration levels reach  $10^{-16} \text{ cm}^2$ .

As seen in figure 2, in spontaneous emission following the excitation of the considered levels by electron impact, the studied upper nonet levels are combined with both nonets  $^9D^\circ$  and  $^9F^\circ$ , and also with the septet term  $^7D^\circ$  and undecuplet  $^{11}F^\circ$ , that is, there are intercombination transitions. In this case, the high-placed upper levels are combined with all the low-lying odd levels shown in figure 2, whereas transitions from  $4f^7(^8S^\circ) 5d(^9D^\circ) 6s 6p(^3P^\circ) ^9F$  term levels end only at the ground term levels. Apparently, this situation is due to the fact that the excitation cross sections of the transitions from the levels of the term  $^9F$  to the levels of the term  $4f^7(^8S^\circ) 5d 6s^2 ^7D^\circ$  are very small, since none of these transitions is registered in [12], in which the transition probabilities are measured for 1290 spectral lines of the gadolinium atom in the wavelength range  $\lambda = 300\text{-}1850 \text{ nm}$ .

**Table 2.** Comparison of the GdI excitation cross-sections

$\lambda$ (nm)	(Å)	Upper level	$E_{\text{up}}$ ( $\text{cm}^{-1}$ )	$Q_{30}$ ( $10^{-18} \text{ cm}^2$ )		Q[Pres.pap.]/Q[3]
				[Pres.pap.]	[3]	
422.585	4226	$4f^7 5d(^9D^\circ) 6s 6p(^1P^\circ) ^9F_7$	25376	91.4	5.05	18.1
426.012	4260*	$4f^7 5d(^9D^\circ) 6s 6p(^1P^\circ) ^9F_5$	23999	26.6	2.64	10.9
426.208	4262	$y^{11}D_5$	30242	2.15		
431.384	4313.8	$4f^7 5d(^9D^\circ) 6s 6p(^1P^\circ) ^9F_3$	23389	78.8	3.17	24.9
432.569	4325	$4f^7 5d(^9D^\circ) 6s 6p(^1P^\circ) ^9F_4$	23644	90.0	5.5	33.7
432.710	4327	$y^9F_1$	23103	89.1		
432.958	4329	$y^{11}D_4$	29876	6.00		
434.645	4346.6	$4f^7 5d(^9D^\circ) 6s 6p(^1P^\circ) ^9F_5$	23999	134.	10.3	18.1

434.662	4346.5 *	$4f^7 5d(^9D^{\circ}) 6s 6p(^1P^{\circ}) ^9F_2$	23215	52.2		
437.384	4373.8	$4f^7 5d(^9D^{\circ}) 6s 6p(^1P^{\circ}) ^9F_3$	23389	48.5	1.08	44.8
440.185	4402	$4f^7 5d(^9D^{\circ}) 6s 6p(^1P^{\circ}) ^9F_6$	24430	42.5	2.01	24.6
440.313	4403	$y^{11}D_6$	30652	6.86		
441.474	4414.7	$4f^7 5d(^9D^{\circ}) 6s 6p(^1P^{\circ}) ^9F_4$	23644	29.5	3.96	9.26
441.416	4414.2 *	$y^{11}D_7$	31146	7.17		
Average						23.05

The results obtained can be compared with the results of [3]. This comparison is given in the table 2. Since the spectral resolution in [3] is several times worse than in the present work, in five cases out of eight the results in [3] are presented by blends. For blend participants, designations of level transitions from which are not considered in this paper are given according to [3]. Asterisks in the second column (as in the work [3] itself) indicate lines that the authors of the work [3] consider to be more intense in blends. In case the line  $\lambda = 422.585$  nm there is a misprint in [3]: instead 4226, specified 4246.

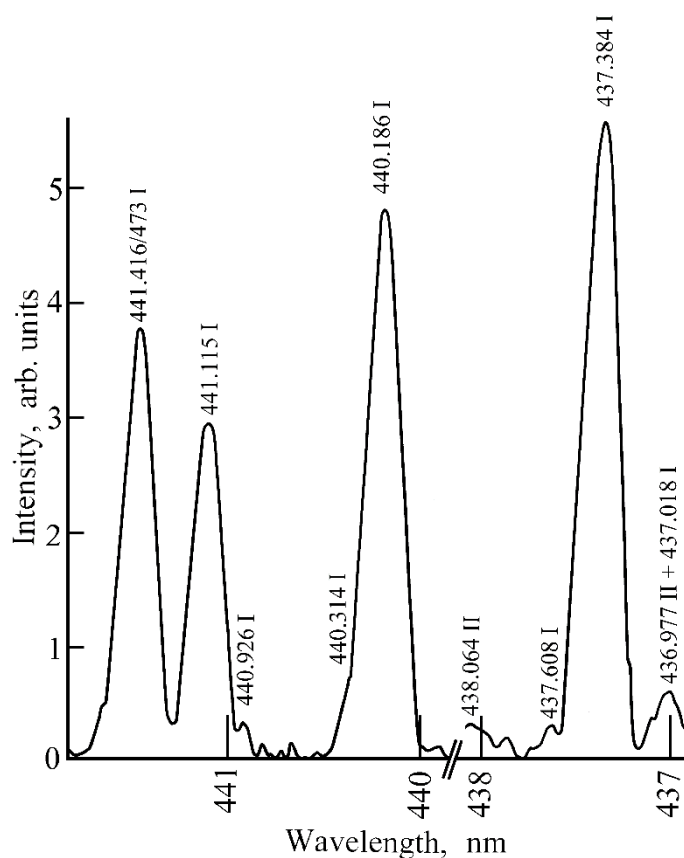


**Figure 3.** Part of spectrogram of the gadolinium (GdI and GdII lines)

As seen in table 2, in all cases, the excitation cross-sections in [3] are substantially less than in the present work. Especially for the line  $\lambda = 437.384$  nm, for which the ratio  $Q[\text{Pres.pap.}]/Q[3] = 44.8$ . When this line is taken into account, the average value of the ratio  $(Q[\text{Pres.pap.}]/Q[3])_{\text{aver}} = 23.05$ , whereas without this line  $(Q[\text{Pres.pap.}]/Q[3])_{\text{aver}} = 19.95$ . The cross-section value for the line  $\lambda = 437.384$  nm in [3] is significantly understated and is 2–4 times less than for closely spaced blends  $\lambda = 4402/3$  and  $4414.7/2$  nm. Parts of the spectrogram for these blend and the line  $\lambda = 437.384$  nm, shown in figure 3. It can be seen that the ratio of peaks on the spectrogram is the same as the ratio of cross sections in the table 1 in this paper (the difference in spectral sensitivity of the installation within the spectral regions shown in figure 3, is very little). This ratio is the same for all registered spectrograms. As for the difference in the scale of the absolute values of the cross sections in this work and in [3] by almost 20 times, the most probable cause of this difference is the method for the concentration of atoms determining in the work [3], in which, however, there is no indication of how this concentration was measured.

#### 4. SUMMARY

In addition to practical problems, some of which are listed in the Introduction, the study of inelastic collisions of electrons with gadolinium atoms is also of interest for the theory of atomic structure. Along with cerium and lutetium, gadolinium is among the three REEs, for which appears 5d electron in the ground state. With half-filled 4f shell, gadolinium has the largest multiplicity of the ground state among all elements – nonet. The associated regularities and peculiarities of excitation processes require systematic study, accumulation, and analysis of information. Unfortunately, to date, there is no theoretical consideration of the excitation of gadolinium atoms by electron impact, which significantly limits the possibility of analyzing the results, obtained in the experiment.

#### References

1. T.A. Ryabchikova, I.S. Savanov, A.P. Hatzes, W.W. Weiss, and G. Handler. Abundance analyses of roAp stars VI. 10 Aql and HD 122970\*. *Astron. Astrophys.*, **357**, 981 (2000)
2. C.R. Cowley, T.A. Ryabchikova, F. Kupka, D.J. Bord, G. Mathys and W.P. Bidelman. Abundances in Przybylski's star. *Mon. Not. R. Astron. Soc.*, **317**, 299 (2000)
3. L.L. Shimon, I.V. Kurta, I.I. Garga. Experimental study of the effective cross-sections of gadolinium atom spectral lines by electron impact. *Opt. Spectrosc.*, **56**, 601 (1984) (in Rus.)
4. Yu.M. Smirnov. Excitation of the gadolinium atom undecuplet levels, belonging to  $4f^5d^26p$  configuration. *Opt. Spectrosc.*, **114**, 492 (2013) DOI:10.1134/S0030400X1304019X
5. Yu.M. Smirnov. Excitation by Electron Impact of Quintet and Septet Levels of Gadolinium Atom Belonging to  $4f^65d6s$  Configuration. *Intern.Rev.Phys.*, **10**, 10
6. Yu.M. Smirnov. Excitation of gallium one-charged ion in e-Ga collisions. *J. Phys. B: At. Mol. Opt. Phys.*, **48**, 165204 (2015) DOI:10.1088/0953-4075/48/16/165204
7. Yu.M. Smirnov. TIII excitation cross-sections in collisions of slow electrons with thallium atoms. *J. Phys. B: At. Mol. Opt. Phys.*, **49**, 175204 (2016) DOI:10.1088/0953-4075/49/17/175204
8. R.K. Peterkop. Calculation of the excitation cross-sections and oscillator strengths of vanadium and manganese atoms. *Opt. Spectrosc.*, **58**, 14 (1985) (in Rus.)
9. Yu. Ralchenko, A.E. Kramida, J. Reader and NIST ASD Team (2008). *NIST Atomic Spectra Database* (version 3.1.5), [Online]. Available: <https://physics.nist.gov/asd3> [2010, May 7]. National Institute of Standards and Technology, Gaithersburg, MD.

10. S.M. Afzal, A. Venugopalan, S.A. Ahmad. Isotope shift studies in the spectra of Gadolinium in UV region and term shift of high even levels of GdI. *Z. Phys. D*, **41**, 95 (1997)
11. B.K. Ankush and M.N. Deo. Fourier transform high-resolution spectroscopic studies of GdI: optical isotope shifts in the spectral region of 18700–20200  $\text{cm}^{-1}$ . *Phys. Scripta*, **81**, 055301 (2010) DOI:10.1088/0031-8949/81/05/055301
12. J.E. Lawler, K.A. Bilty and E.A. Den Hartog. Atomic transition probabilities of GdI. *J. Phys. B: At. Mol. Opt. Phys.*, **44**, 095001 (2011) DOI:10.1088/0953-4075/44/9/095001